The ferromagnetic moment of an antiferromagnetic domain wall

1998 J. Phys.: Condens. Matter 10 L131

(http://iopscience.iop.org/0953-8984/10/8/004)

J. Phys.: Condens. Matter **10** (1998) L131–L138. Printed in the UK PII: S0953-8984(98)88823-1

LETTER TO THE EDITOR

The ferromagnetic moment of an antiferromagnetic domain wall

N Papanicolaou

Department of Physics, University of Crete, and Research Centre of Crete, Heraklion, Greece

Received 28 October 1997, in final form 26 January 1998

Abstract. We present a theoretical study of an Fe/Cr multilayer film which may be thought of as a synthetic antiferromagnetic superlattice. We clarify certain aspects of the surface-spin-flop transition in which a domain wall nucleates at the outer layer and eventually migrates to the centre with increasing bias field. In particular, the nonvanishing ferromagnetic moment predicted earlier for bulk domain walls at vanishing field is shown to drive a prolonged hysteresis cycle and could thus be detected experimentally.

Domain walls that may occur in the bulk of a classical antiferromagnetic chain were recently shown to exhibit a nonvanishing total magnetic moment which approaches the values $\pm s$, in the limit of weak easy-axis anisotropy, where s is the magnitude of the classical spin at each lattice site [1]. This curious result would appear to be rather academic for crystalline antiferromagnets, in view of the miniscule (atomic) values of s, even though it could play some role within a proper semiclassical quantization of antiferromagnetic domain walls [2]. Nonetheless the picture changes drastically in the case of an antiferromagnetic superlattice, such as Fe/Cr, because the local moment s coincides with the ferromagnetic moment of each Fe layer and thus acquires macroscopic size. As a consequence, the superlattice is effectively described by a classical spin chain whose sites correspond to the Fe layers and the exchange coupling between adjacent layers is antiferromagnetic for Cr thickness in the neighbourhood of 11 Å.

The essential ingredient of the scenario demonstrated both theoretically and experimentally in [3] is a surface-spin-flop (SSF) transition that takes place on a finite superlattice. When the bias field exceeds a certain critical value, which is smaller than the critical field required for the familiar bulk spin-flop (SF) transition roughly by a factor $\sqrt{2}$, a domain wall nucleates near one of the two free ends of the superlattice. With further increase of the applied field the domain wall migrates to the centre and subsequently expands more or less symmetrically to approach a SF state that is nearly uniform within the bulk. The SF state eventually saturates to complete ferromagnetic order after the field exceeds yet another critical value.

The above rough description of the SSF transition glosses over some important details concerning the process of nucleation of a domain wall. Our first aim is to examine more closely the formation of the true SSF state advocated in [4] which proceeds by a first-order transition and provides the true hysteresis curve when the cycle is reversed carefully. However the generic hysteresis curves obtained in a variety of simulations [5, 6] are significantly different and may extend all the way down to vanishing field. We shall argue here that a prolonged hysteresis cycle is driven by a domain wall trapped near the

0953-8984/98/080131+08$19.50

centre, whose total moment remains finite even at vanishing field, and should be a robust feature of antiferromagnetic superlattices. In turn, such a scenario may provide a method for the experimental detection of the theoretically predicted ferromagnetic moment of an antiferromagnetic domain wall [1].

We consider a finite superlattice (chain) with Λ layers (sites). The yz plane is taken to coincide with the plane of each layer and is thus perpendicular to the chain, x direction. The ferromagnetic moment of each Fe layer is described by a spin $\boldsymbol{S}_i$, residing at the site $i = 1, 2, \ldots, \Lambda$ of the equivalent chain, which carries constant magnitude s ($\boldsymbol{S}_i^2 = s^2$) and satisfies the classical Landau–Lifshitz equation [7] adapted to the present problem [1], namely

$$\begin{aligned}(1+s^2\gamma^2)\frac{\partial \boldsymbol{S}_i}{\partial t} &= (\boldsymbol{S}_i \times \boldsymbol{F}_i) - \gamma[\boldsymbol{S}_i \times (\boldsymbol{S}_i \times \boldsymbol{F}_i)] \\ \boldsymbol{F}_i &= -J(\boldsymbol{S}_{i+1} + \boldsymbol{S}_{i-1} - 2\boldsymbol{S}_i) - (K_1 S_i^x \boldsymbol{e}_1 - K_3 S_i^z \boldsymbol{e}_3) + H\boldsymbol{e}_3\end{aligned} \tag{1}$$

where $\boldsymbol{e}_1$, $\boldsymbol{e}_2$ and $\boldsymbol{e}_3$ are unit vectors along the three axes. The exchange term in the effective field $\boldsymbol{F}_i$ should be completed with the stipulation that it contain only one spin when applied for the outer layers; $i = 1$ or Λ. The anisotropy term is such that the easy or z axis lies within each layer, while the hard or x axis points along the chain direction thanks to the effect of the magnetostatic field at low frequencies [5]. The last term in $\boldsymbol{F}_i$ is the contribution of a uniform external field applied along the easy axis.

The spin magnitude s and the exchange constant J may be scaled out of the calculation and the relevant parameters are the rationalized easy-axis anisotropy and bias field defined from

$$\varepsilon = \sqrt{\frac{K_3}{J}} \qquad h = \frac{H}{2\varepsilon s J} \tag{2}$$

as well as the dimensionless hard-axis anisotropy K_1/J and dissipation constant $s\gamma$. The most important parameter is the easy-axis anisotropy for which we shall mainly use a value $\varepsilon = 1/2$ that is typical in Fe/Cr superlattices. It is also significant that $h = 1$ corresponds to a modest magnetic field in the vicinity of $H \sim 1$ kG. On the other hand, a precise specification of K_1/J and $s\gamma$ is not necessary for the current work. These parameters are relevant for some transient dynamical details but do not affect the shape of the equilibrium spin configurations which ultimately develop in the yz plane. For definiteness, we have employed the value $K_1/J = 21$ recommended in [5] and have adopted a relatively large dissipation constant $s\gamma = 1$ that leads to relaxation essentially within a few rationalized time units, defined as $\tau = 2\varepsilon s J t$. In fact, if one only aims at locating the energy minima, one may use a very large dissipation constant so that the precession term in equation (1) can be neglected and

$$\frac{\partial \boldsymbol{S}_i}{\partial t'} = -\boldsymbol{S}_i \times (\boldsymbol{S}_i \times \boldsymbol{F}_i) \tag{3}$$

where t' is a suitably rescaled pseudotime variable. The advantage of the fully dissipative equation (3) is that it rapidly leads to equilibrium [1], whereas equation (1) describes a physical process that is closer to what is actually done in an experiment. Our main results presented in the following were confirmed using both equation (1) and (3).

Now assume that a superlattice with an even number of layers ($\Lambda = 20$) is initially relaxed in its ground (Néel) state shown in the first row of figure 1 at vanishing field. Our task is to predict the fate of the ground state after a finite field h is turned on. Actually the pure Néel state is an exact static solution of equation (1) for any value of the applied field. Hence we study the stability of the Néel state in the presence of a random perturbation.

We consider first the case of a 'small' perturbation simulated here by replacing the value $\boldsymbol{S}_\Lambda = s(0, 0, -1)$ of the rightmost spin with, say, $\boldsymbol{S}_\Lambda = s(0, 0.14, -0.99)$. (In practice, a disturbance of this nature may be realized by temporarily applying a small in-plane field near the surface of the superlattice in a direction perpendicular to the easy axis.) We then view the perturbed state as the initial condition and numerically calculate its time evolution through equation (3). Not surprisingly, such a state quickly relaxes back to the pure Néel state when the bias field h is sufficiently small. This result is consistent with the fact that the anticipated bulk SF transition should occur only when the field exceeds a certain (rationalized) critical value in the neighbourhood of $h \sim 1$; the precise value may be found in equation (4.17) of [1] and reduces to $h = 1$ in the weak-anisotropy limit $\varepsilon \to 0$.

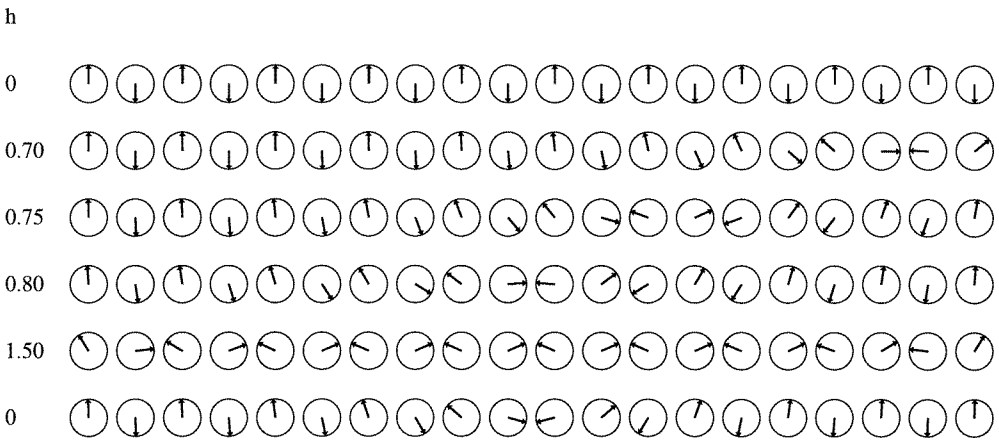

Figure 1. Snapshots of the SSF transition at various values of the field h. The relaxed spin configurations are confined in the yz plane which is rotated onto the plane of the figure.

Nevertheless a detailed search in steps of $\delta h = 0.01$ reveals that the Néel state is rendered unstable at an earlier stage, namely when $h = h_2 \approx 0.75$. The corresponding relaxed configuration, shown in the third row of figure 1, clearly demonstrates that a domain wall has suddenly appeared somewhere between the rightmost layer and the centre of the superlattice. This result agrees with the calculation of [3]; so does the subsequent evolution of the domain wall calculated here by continuing the procedure beyond $h = 0.75$, also in steps of $\delta h = 0.01$, using as initial condition at each step the relaxed configuration obtained in the preceding step. The wall has practically moved to the centre at $h = 0.80$, as shown in the fourth row of figure 1, but a slight asymmetry around the centre persists in the numerical data beyond the eighth significant figure. The asymmetry is progressively reduced at higher fields, as the wall expands around the centre, and disappears for $h \gtrsim 1$ within machine (16-place) accuracy. Meanwhile the domain wall gradually turns into a uniform SF state within the bulk, with notable nonuniformities around the edges, as is apparent in the case $h = 1.5$ depicted in the fifth row of figure 1. Further increase of the applied field eventually leads to complete ferromagnetic order which first occurs when $2\varepsilon h = 4 - \varepsilon^2$; in our calculation $\varepsilon = 1/2$ and $h = 3.75$. The described process is also monitored in figure 2 which plots the field dependence of the total magnetic moment $\boldsymbol{\mu} = \sum_i \boldsymbol{S}_i = (\mu_1 = 0, \mu_2, \mu_3)$ by a solid line. The solid curve for μ_3 is in general agreement with the result of [3], while the small component μ_2 that develops along the y axis in a narrow field regime above $h_2 = 0.75$ provides a measure of the asymmetry of the wall around the centre and practically disappears for $h > 0.80$.

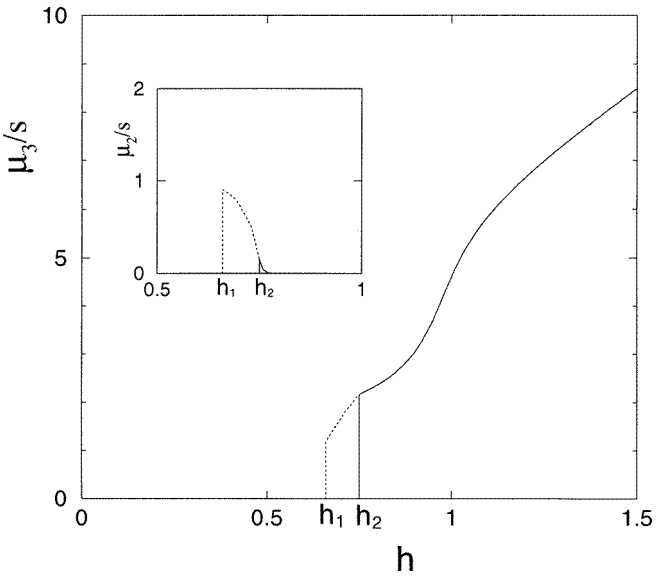

Figure 2. The field dependence of the total magnetic moment $\boldsymbol{\mu} = (\mu_1 = 0, \mu_2, \mu_3)$ depicted by solid and dotted lines corresponding to the two applied field sequences.

The procedure followed above suggests that h_2 is the characteristic field where a surface-spin-wave mode turns soft [8] and hence the Néel state becomes unstable to small perturbations for $h > h_2$. Indeed, an examination of small fluctuations of the Néel state on a semi-infinite chain yields the field value

$$h_2 = \frac{1}{2}\sqrt{2+\varepsilon^2} \tag{4}$$

which reduces to $h_2 = 1/\sqrt{2}$ in the limit of weak anisotropy ($\varepsilon \to 0$) but gives $h_2 = 3/4$ for $\varepsilon = 1/2$. The very slight departure from the above value observed in our simulation is due to the finiteness of the lattice ($\Lambda = 20$). One should also mention that the field h_2 given in equation (4) coincides with the field determined from equation (3) of [4] obtained through a different reasoning and thought to provide the phase boundary of the AF_3:AF_4 transition.

In the present context, the sudden appearance of a domain wall within the chain, the sudden jump of the total moment and a corresponding sudden reduction of the energy make it clear that the SSF transition is first order and could occur at a field smaller than h_2. In order to probe for such a possibility we repeat the procedure by invoking a 'large' fluctuation in the initial Néel state, implemented here by nearly flipping the spin of the outer layer from its Néel value $\boldsymbol{S}_\Lambda = s(0, 0, -1)$ to, say, $\boldsymbol{S}_\Lambda = s(0, 0.14, 0.99)$. Such an initial condition no longer relaxes to the pure Néel state, when the field exceeds the value $h_1 \approx 0.66$, but to a nontrivial surface state illustrated in the second row of figure 1 for $h = 0.70$. Clearly this is the SSF state discussed in [4] in which the outer spin forms an angle with the easy axis approximately equal to 60°. One should also note that the SSF state comes in two varieties distinguished by their handedness. Had we started with the initial condition $\boldsymbol{S}_\Lambda = s(0, -0.14, 0.99)$ the outer spin would have again tilted by nearly 60° but to the left of the easy axis. When the field is increased to approach the value $h_2 = 0.75$, the SSF state evolves into the domain wall shown in the third row of figure 1 and, thereafter, the process

continues as described earlier in the text. As a consequence, the total moment of the SSF state, depicted by a dotted line in figure 2, joins smoothly with the earlier results at $h = h_2$. The observed sizable component μ_2 implies that the SSF state is significantly twisted.

A closer look at the numerical energy data reveals that we are dealing with a genuine first-order transition characterized by three distinct field values ordered as $h_1 < h_c < h_2$, where $h_1 \approx 0.66$ and $h_2 \approx 0.75$ are the fields already discussed. The low-energy regime may be envisaged roughly as an uneven double well whose two local minima correspond to the Néel and SSF states. The Néel state is locally stable for $h < h_2$ and the SSF state for $h > h_1$. The energies of the two minima coincide at $h = h_c = 0.682\ldots$ which lies in the overlaping domain $[h_1, h_2]$. The SSF state first appears as a metastable local minimum in the region $[h_1, h_c]$ and becomes the absolute minimum for $h > h_c$. Similarly the Néel state is the absolute minimum for $h < h_c$ and survives as a metastable local minimum in $[h_c, h_2]$. Therefore, strictly speaking, the true SSF transition occurs at the critical field h_c. Nevertheless all three characteristic field values are important in connection with hysteresis. One should further note that the two states discussed above are not the only local minima of the energy functional. On the contrary, a multitude of metastable minima are present with energies that differ only slightly. The implied chaotic behaviour of this fascinating system was already emphasized in the earlier work, especially in [9], and is also important for the ensuing discussion of hysteresis.

The preceding description of the 'true SSF transition' establishes that the 'true hysteresis loop' is given by the solid and dotted lines of figure 2 taken in combination. Specifically, let us invoke the original scenario and drive the system to a nominal field h_0, just above h_2, where a domain wall appears within the chain but is still off centre. If we then reverse the cycle carefully, by reducing the applied field adiabatically, the wall returns to the rightmost layer, through the formation of a SSF state in reverse order, and finally exits the system at $h = h_1$ where the chain returns to the pure Néel state. Consequently the total moment retraces the dotted lines of figure 2 also in reverse order.

However the hysteresis loop of figure 2 is far from generic when the nominal field h_0 is taken to be sufficiently large, practically in the region $h_0 > 0.8$, where the relaxed spin configuration is symmetric around the centre to great numerical precision. If we use such a configuration as initial condition in equation (1), and then reduce the field adiabatically, the calculated hysteresis curve is rather prolonged and typically extends all the way down to vanishing field [5, 6]. An example of such a calculation is shown in figure 3 obtained here by a continuous adiabatic field reduction given by $h = h_0 - \alpha\tau$, with $\alpha = 10^{-6}$, and a nominal field $h_0 = 0.9$ or 1.5, both cases leading to essentially the same result depicted by a dashed line. Despite appearances the solid and dashed lines in figure 3 do not join smoothly at h_2. The small discrepancy illustrated in the inset of the same figure is certainly not due to numerical imprecision but reflects the important fact that a domain wall is trapped near the centre of the chain during the descending side of the cycle. Such a fact is corroborated by monitoring the corresponding spin configuration. In particular, when the field is completely switched off ($h = 0$) the resulting configuration, shown in the sixth row of figure 1, is simply the bulk domain wall illustrated earlier in figure 1 of [1]. A related interesting fact is that the same domain wall is realized by *suddenly* turning off the field h_0 and then letting the configuration relax through equation (1) or (3). If we further reverse the cycle once again, by increasing the field adiabatically, the dashed line of figure 3 is reproduced.

The key element of this calculation is that the relaxed spin configuration at some field h_0 loses memory of its history when h_0 is sufficiently large. As mentioned earlier, memory is stored in a slight asymmetry of the relaxed configuration, which is lost to within 16-place accuracy when $h_0 \gtrsim 1$. But even when $0.8 \lesssim h_0 \lesssim 1$, the asymmetry is pushed beyond the

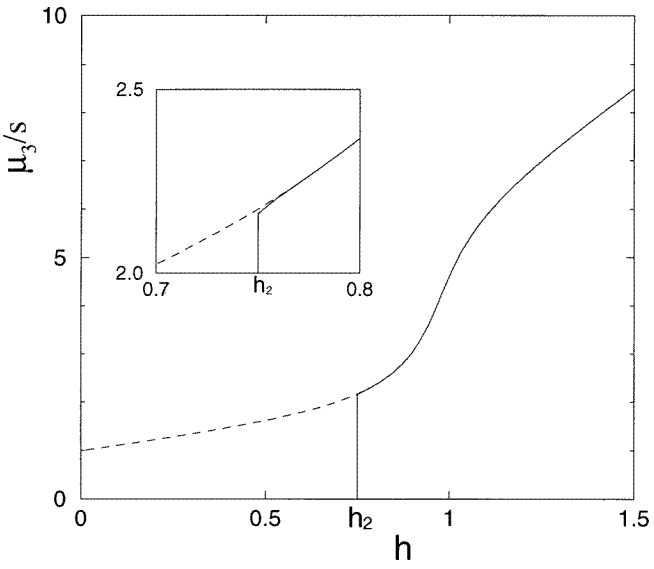

Figure 3. The generic hysteresis curve (dashed line) obtained by reversing the cycle after the spin configuration had relaxed at the nominal field value $h_0 = 1.5$. The dashed line is indistinguishable from the corresponding solid line of figure 2 *almost* down to the field value $h_2 = 0.75$, as shown in the inset.

eighth significant figure and is apparently washed out by small errors made at each step of the numerical integration of equation (1) during the descending side of the cycle. On the assumption that random numerical errors may provide a genuine representation of noise in a realistic superlattice, one must conclude that the spin configuration loses its memory as it descends through the Rubikon of fields near the SSF transition and, thereby, is locked into a high-energy local minimum which is a bulk domain wall trapped at the centre.

Whereas a firm theoretical explanation of the picture outlined above is lacking, one may nonetheless provide a semi-analytical description of the prolonged hysteresis curve of figure 3 based on the continuum approximation of bulk domain walls worked out in [1]. At first sight, it appears improbable that a continuum description can be useful for such a short chain ($\Lambda = 20$) and strong anisotropy ($\varepsilon = 1/2$) because there exist two competing conditions for its validity: (a) the wall must be sufficiently wide to allow a formulation in terms of continuous functions and (b) the wall must be sufficiently narrow to fit within a finite chain. The discussion of [1] suggests that these conditions are equivalent to the strong inequalities

$$1/\Lambda \ll \varepsilon\sqrt{1-h^2} \ll 1 \tag{5}$$

which are meaningful in the region $h < 1$; i.e., below the critical field $h = 1$ of the bulk SF transition in the limit of weak anisotropy. The total moment of a domain wall is then given analytically by

$$\mu_1 = 0 = \mu_2 \qquad \mu_3 = s\left[1 + \frac{h}{\sqrt{1-h^2}}\right]. \tag{6}$$

Interestingly, both inequalities in equation (5) are reasonably satisfied in our current example when $h < 1$. Therefore, if we recall that the prolonged hysteresis curve (dashed line) of figure 3 also describes the total moment of a domain wall trapped near the centre, we

conclude that such a curve can be approximated by equation (6). Indeed, in figure 4, we observe a reasonable agreement for $h < 1$; of course, the two curves diverge from each other as h approaches unity because the left inequality in equation (5) is then violated or, equivalently, the domain wall expands and clearly senses the boundaries of the finite chain. We have repeated the calculation for a larger superlattice ($\Lambda = 200$) and a weaker anisotropy ($\varepsilon = 0.1$), a choice that strengthens both inequalities in equation (5). One would thus expect that the agreement should improve for any given value of h, in the region $h \lesssim 1$, as actually demonstrated in the inset of figure 4.

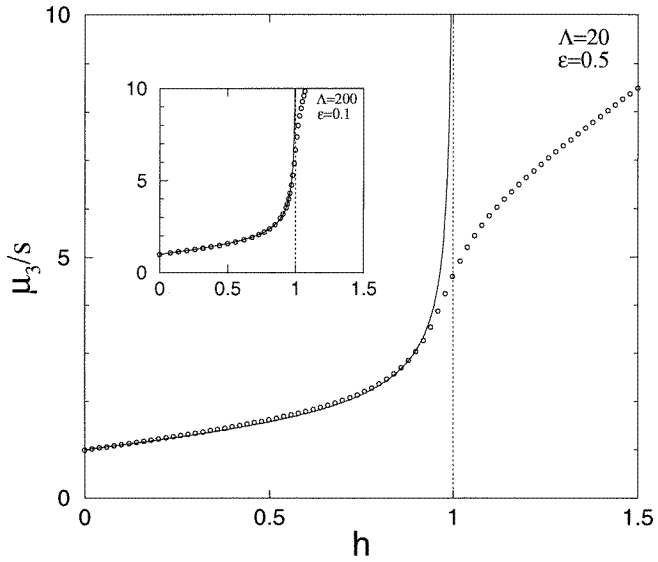

Figure 4. Comparison of the generic hysteresis curve of figure 3, now depicted by open circles, to the analytical prediction of equation (6) shown by a solid line. The main figure illustrates the results for our standard choice of parameters, $\Lambda = 20$ and $\varepsilon = 1/2$, while the inset for $\Lambda = 200$ and $\varepsilon = 0.1$.

The published experimental data [5] on hysteresis in Fe/Cr do not seem to be sufficiently detailed or accurate to resolve at this point the finer issues discussed in the present letter. In this respect, one should keep in mind that Kerr measurements may not be entirely appropriate because they probe mostly the outer layers, whereas it is difficult, if not impossible, to ascertain where the total ferromagnetic moment of an antiferromagnetic domain wall is actually located [10]. Putting it differently, the local distribution of the ferromagnetic moment is somewhat elusive, a fact reflected in the appearance of parity-breaking contributions within a continuum description. Nevertheless the total moment is completely unambiguous and should be amenable to experimental detection. One should further mention that domain walls may occur also in the bulk of a superlattice with an odd number of layers, and their total moment differs from that of the ground state by an amount $\pm s$ in the limits of weak anisotropy and vanishing field. However domain walls cannot be produced on an odd superlattice via a SSF transition [3].

We conclude with a few comments on the numerical integration of equations (1) and (3). One would think that resolving the constraint $\boldsymbol{S}_i^2 = s^2$ through, say, a spherical parametrization should expedite the process. Actually such a parametrization introduces artificial coordinate singularities when a spin approaches the north or the south pole, a frequent occurrence in this problem, which put a strain on the calculation. Instead, we

found it far more efficient to look upon the Landau–Lifshitz equation as a system of three equations, one for each spin component, and re-enforce the constraint after every time step of the numerical integration. This trick was borowed from earlier calculations in the nonlinear σ model [11]. One may then use a standard Runge–Kutta algorithm for the time integration. In fact, even a straightforward first-order time differencing scheme proves to be stable for all calculations presented here, provided that the time step is chosen in the neighbourhood of 10^{-2}. The required CPU time is rather insignificant. For example, complete relaxation at a specific field value is typically obtained through equation (3) using 10^6 time steps which amount to less than one minute on a modest HP715 workstation.

I am indebted to D L Mills for sending me a copy of [5] prior to publication, and to C Micheletti for a copy of his Oxford DPhil thesis.

References

[1] Papanicolaou N 1995 *Phys. Rev.* B **51** 15 062
[2] Ivanov B A and Kolezhuk A K 1995 *Phys. Rev. Lett.* **74** 1859
[3] Wang R W, Mills D L, Fullerton E E, Mattson J E and Bader S D 1994 *Phys. Rev. Lett.* **72** 920
[4] Micheletti C, Griffiths R B and Yeomans J M 1997 *J. Phys A: Math. Gen.* **30** L233
[5] Rakhmanova S, Mills D L and Fullerton E E 1997 Low frequency dynamic response and hysteresis in magnetic superlattices *Preprint*
[6] Wang R W and Mills D L 1994 *Phys. Rev.* B **50** 3931
[7] Landau L and Lifshitz E 1935 *Physik* A **8** 153
[8] Mills D L and Saslow W 1968 *Phys. Rev.* **171** 488
[9] Trallori L, Politi P, Rettori A, Pini M G and Villain J 1994 *Phys. Rev. Lett.* **72** 1925
Trallori L, Politi P, Rettori A, Pini M G and Villain J 1995 *J. Phys.: Condens. Matter* **7** L451
[10] Papanicolaou N 1997 *Phys. Rev.* B **55** 12 290
[11] Leese R A, Peyrard M and Zakrzewski W J 1990 *Nonlinearity* **3** 773